Ecological Informatics 92 (2025) 103444

Contents lists available at ScienceDirect

Ecological Informatics

journal homepage: www.elsevier.com/locate/ecolinf

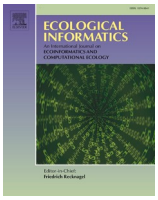

Habitat mapping of coastal dunes with deep learning

Eva M. Lansu [a,b,*], Valérie C. Reijers [c], Freek Daniëls [d], Rebecca James [e], Marjolijn J.A. Christianen [e], Tjisse van der Heide [a,b]

[a] Department of Coastal Systems, Royal Netherlands Institute for Sea Research (NIOZ), Den Burg, the Netherlands
[b] Conservation Ecology Group, Groningen Institute for Evolutionary Life Sciences, University of Groningen, Groningen, the Netherlands
[c] Faculty of Geosciences, Department of Physical Geography, Utrecht University, Utrecht, the Netherlands
[d] Wageningen Food and Biobased Research, Wageningen, the Netherlands
[e] Aquatic Ecology and Water Quality Management Group, Wageningen University & Research, Wageningen, the Netherlands

ARTICLE INFO

Keywords:
Convolutional neural network
U-net
Semantic segmentation
Dune habitats
Vegetation mapping

ABSTRACT

About one-third of the world's shoreline is defined by sandy coasts with developed dune ecosystems. These ecosystems have drastically degraded due to anthropogenic pressures. To develop strategic management that counteracts this degradation, it is essential to closely monitor ongoing habitat changes. Traditionally, coastal dune monitoring is based on field observations, which are labour intensive and costly. While automated analyses of aerial imagery could reduce monitoring efforts and enhance spatial coverage, to date, its application has remained limited to a single small-scale trial (<2 km^2). Here, we trained a Convolutional Neural Network to map the Dutch coastal dunes (562 km^2) at 25 cm resolution using six habitat classes: bare sand, shrubs, fresh water, grass, broadleaf trees, and needleleaf trees. Training the network on only RGB imagery resulted in predictions with 92 % accuracy, 80 % average recall and 70 % precision. Model performance increased when the network was trained on all available data – RGB imagery, near-infrared, distance to sea, digital surface model, and canopy height - resulting in 95 % accuracy, 88 % averaged recall and 80 % precision. Finally, we compared the predictions with 499 in-field observations across the Dutch coastal dunes and found 88 % accuracy, 74 % averaged recall and 62 % precision. We used this model to create a map of the entire Dutch coastal dunes, which enables rapid and precise assessments of habitat diversity and extent. As habitat and species diversity are intrinsically linked, our results showcase how automated image analysis can enable biodiversity monitoring on a national scale.

1. Introduction

About one-third of the world's shoreline is defined by sandy coasts with developed dune ecosystems (Luijendijk et al., 2018; Martínez et al., 2004). These coastal dune systems provide vital services to humans as they protect against flooding, provide tourism opportunities, and are able to purify water to drinking standards (Barbier et al., 2011; Drius et al., 2019). However, anthropogenic pressures, such as infrastructure development and land-use change, have increasingly reduced and fragmented the spatial extent of coastal dunes (Delgado-Fernandez et al., 2019; Hilton, 2006; Lansu et al., 2024; Lu et al., 2018; Sperandii et al., 2021). Consequently, 86 % of the coastal dune habitats in Europe have a poor to bad conservation status, with over half showing a deteriorating trend (Naumann et al., 2020). The observed degradation of European dune habitat has been related to enhanced vegetation cover – called 'greening' of the coastal dunes (Gao et al., 2020; Jackson et al., 2019; Jackson and Cooper, 2011; Petrova et al., 2023). It leads to the loss of open dune habitat, and thereby it homogenizes the dune landscape (Pye et al., 2014; Pye and Blott, 2017). As a direct consequence, many rare plants, invertebrates and other species that require open, mobile sands decline or go extinct (Bird et al., 2017; Pye et al., 2014). This trend is concerning, not only because the decline in biodiversity affects ecosystem functioning (Chapin et al., 1998), but also because enhanced vegetation cover has been associated with a decreased capacity of coastal dunes to grow vertically with sea-level rise (Arens et al., 2020). To mitigate the trend of dune habitat losses and degradation, it is desirable to effectively monitor the changing dunes at landscape scale.

The importance of monitoring the habitat quality status of coastal dunes is well recognized, as large coordinated networks of protected areas, such as Natura 2000 (covering 18 % of the land in the EU),

* Corresponding author at: Department of Coastal Systems, Royal Netherlands Institute for Sea Research (NIOZ), P.O. Box 59, 1790 AB Den Burg, the Netherlands.
E-mail address: eva.lansu@nioz.nl (E.M. Lansu).

https://doi.org/10.1016/j.ecoinf.2025.103444
Received 8 April 2025; Received in revised form 22 September 2025; Accepted 24 September 2025
Available online 25 September 2025

obligate monitoring of their conservation status (Delbosc et al., 2021; Röschel et al., 2020). However, the large spatial heterogeneity of dune landscapes and their dynamic nature complicate monitoring efforts. In a natural dune system, large-scale and small-scale gradients interact, creating a highly diverse landscape. On the large scale, decreasing sand deposition and flooding frequency create a gradient of decreasing stress in the landward direction (Lane et al., 2008; McLachlan, 1991; Ruocco et al., 2014). On the smaller scale, across dune slopes and valleys, variations in soil water content and organic matter create additional spatial heterogeneity. This natural combination of gradients hosts a mosaic of habitat types - consisting of bare sand, shrubs, fresh water, grass, broadleaf trees, and needleleaf trees - which changes composition with distance to sea (Hesp, 2002; McLachlan, 1991; Ruocco et al., 2014). Consequently, to analyse dune vegetation composition, monitoring with large spatial coverage and fine spatial resolution is needed to capture both the large-scale zonation and the small-scale heterogeneity.

Apart from the high spatial variation, also rapid developments over time pose a challenge to dune vegetation monitoring. At the timescale of years to decades, processes such as sedimentation, dune greening, stabilization and succession can substantially change the dune landscape (Gao et al., 2020; Jackson et al., 2019; Jackson and Cooper, 2011; Petrova et al., 2023). To be able to disentangle long-term trends from sudden local impacts, such as the development of infrastructure and management interventions (Lansu et al., 2024), observations should be frequent enough to capture the temporal dynamics of vegetation development. Therefore, to observe general trends of changes in vegetation composition, monitoring should be on a large spatial scale with both a fine spatial and temporal resolution.

Traditionally, changes in vegetation composition and habitat diversity are monitored through field vegetation recordings (Delbosc et al., 2021; van Rooijen et al., 2015). Although field-based mapping is very accurate and detailed on a small-scale, it is costly and time-consuming to implement on a large spatial scale. For example, all Dutch coastal dune areas are protected by Natura 2000. Legislation (the 'Habitat Directive') requires member states of the European Union to monitor the conservation status of habitats and species in these protected areas, and to report the results every 6 years (Alberdi et al., 2019; Maccherini et al., 2020). This monitoring is often done by local nature managers, who search for species within areas of 25*25 m (BIJ12, 2021). In contrast to this field-based mapping, aerial image analysis is less labour-intensive and costly. Additionally, the potential of automated image analysis is boosted by the increasing availability of aerial and satellite imagery, which holds for the hazard-prone coastal zone in particular (Laignel et al., 2023; Melet et al., 2020; Vitousek et al., 2023).

An inherent disadvantage of 'monitoring from above' is the point of perspective. Whereas all vegetation layers can be identified during a field visit, only the upper layer can easily be observed from above. The extracted information from aerial images is therefore typically less detailed on the small-scale, but it can complement in-field observations by providing a full-coverage picture on the large-scale. Recently, the possibilities with aerial image analysis have gained momentum. Several automated mapping methods have been developed, including rule-based and machine-learning based mapping, with deep learning appearing as an especially promising method (Choudhary et al., 2022; Kattenborn et al., 2021; Lecun et al., 2015). This is reflected in a wide range of applications, for instance in mapping for agriculture, water body identification and landslide risk (Attri et al., 2023; Azarafza et al., 2021; Wieland et al., 2023). A specific group of deep learning networks is formed by the Convolutional Neural Networks (CNNs), which are able to recognize complex patterns in images (Choudhary et al., 2022; Kattenborn et al., 2021). The application of CNNs seems therefore suitable for the purpose of identifying dune habitats from aerial imagery. Yet, the application to dune habitat classification has - to our knowledge - remained limited to a single trial in relatively small-scale dune areas ($<2km^2$) with limited habitat variability (Pérez-Carabaza et al., 2021), leaving the question of whether monitoring by machine learning at large spatial scales can complement in-field observations unanswered.

To pave the way for applying deep learning to large-scale coastal dune habitat mapping, we tested whether CNNs can accurately map habitat diversity of the coastal dunes in the Netherlands. We used freely available input data: multispectral aerial imagery, a digital terrain model, a digital surface model and a land use map (Table S1). To estimate the value of the input data layers, we trained U-net on different combinations of input data and computed the accurateness of the predictions based on a test set. Additionally, we computed the 'in-field accuracy', by comparing the U-net predictions with 499 country-wide ground truthing observations. In this paper, we present the results of these analyse and showcase how automated image analysis enables ecosystem monitoring on a national scale.

2. Materials and methods

We developed a deep learning model to conduct automated image analyses on aerial imagery of the Dutch coastal dunes. It was trained to classify the aerial imagery in habitat type classes, such as bare sand and broadleaf forest. The accurateness of its predictions was determined using a test set. Additionally, 'in-field accuracy' was determined using 499 country-wide ground truthing observations. Finally, we used the model to classify the entire Dutch dune area and presented the map in a Google Earth Engine app (Gorelick et al., 2017).

2.1. Data acquisition and preparation

We downloaded several open datasets of the Dutch coastal zone (Fig. 1): orthophoto mosaics including a near-infrared band (25 cm resolution, from http://geotiles.nl/), a digital surface model, a digital terrain model (50 cm resolution, obtained through LiDAR survey, from https://www.ahn.nl/) and a land-use map (5 m resolution, from https://lgn.nl/basiskaart). The aerial imagery, taken from an airplane between 19-04-2020 and 07-08-2020, underwent non-uniform post-processing and colour correction by the provider (pers. comm. with *Beeldmateriaal*). In Table S1, all data sources, including their spatial resolution, are listed. As a first step, to standardize all data layers to a resolution of 25 cm, we resampled the digital surface model, digital terrain model and land-use map using nearest-neighbour interpolation. Using the resampled data, we computed a canopy height map by subtracting the digital terrain model from the digital surface model (Fig. 3). Additionally, we calculated the Euclidean distance to the sea for each 25 cm pixel, based on the location of the sea obtained from the land-use map. We then delineated the boundaries of our study area (i.e. the Dutch coastal dunes) using the land-use map. Specifically, we excluded areas categorized as agriculture, roads, buildings, etcetera (Table S3) by converting them to no-data in all data layers. Next, we stacked the prepared data into images consisting of seven layers: red (i), green (ii), blue (iii), near-infrared (iv), distance to sea (v) digital surface model (vi) and canopy height model (vii).

2.2. Training the network

In the following steps, we explain how we annotated imagery to create training data. With this annotated imagery, we trained a deep learning network to classify the coastal dunes into six habitat classes. We repeated this training on different combinations of input data to test the usefulness of our input data layers.

2.2.1. Creating training data

To train, validate and test the deep learning network, we annotated a subset of 110 aerial images, distributed over the study area. We first randomly selected 100 images from the study area. Then, to ensure an even spatial distribution, we selected 10 extra images from the areas that seemed relatively sparsely sampled. We annotated the images by applying 'semantic segmentation' to categorize each pixel (Garcia-

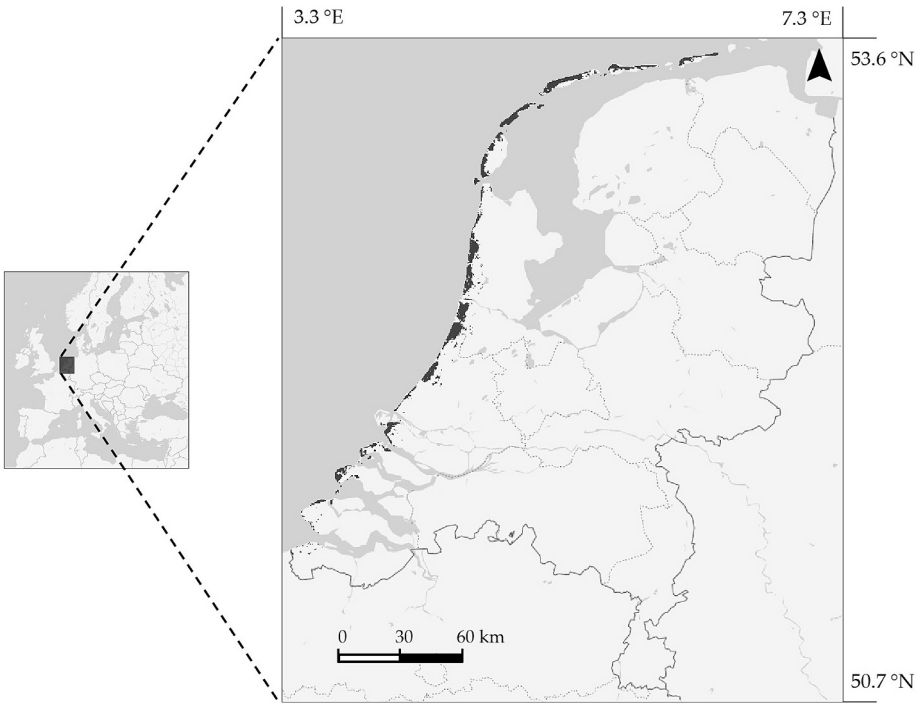

Fig. 1. The coastal dunes of the Netherlands form our study area (depicted in dark grey), which covers 562 km^2 (2 % of the country area). The Netherlands is located in Western Europe (inset).

Garcia et al., 2017) using six classes: bare sand, shrubs, freshwater, grass, broadleaf trees, and needleleaf trees (Fig. 2). Notably, these classes are simplified compared to the Natura 2000 habitat types but can be related to this classification in a straightforward manner (Table S2). As segmenting 110 images fully manually is very tedious, we used unsupervised k-means clustering to segment the main clusters in the multispectral imagery and in the digital surface model. Subsequently, we manually assigned classes to these clusters, using the MATLAB's Statistics and Machine Learning Toolbox version 24.2 (The MathWorks Inc., 2024b). With this methodology, it took one person approximately seven working days to create the training set. In total, the annotated images covered an area of 108 km^2, which equals 12 % of the study area. Next, to reduce computation time, we divided the annotated images into four, which yielded 440 images of 2048*2048 pixels - corresponding to 512*512 m in the real world.

2.2.2. Training, validation and test set

From this set of 440 images, we took a random subset of 264 images (60 %) for training, 88 (20 %) for validation and 88 (20 %) for testing (Fig. S1). This division allowed for a good-sized validation and test set, that represented the spatial variability of the study area (Eelbode et al., 2021), while maximizing the training set. With the training set, the network tuned its parameters, whereby it 'learned' how to recognize the classes. With the validation set, the network learned to avoid underfitting (i.e. the network fails to capture the complexity of the data) and overfitting (i.e. the network 'memorizes' the training data and cannot generalize enough) during the training process. Lastly, with the test set we evaluated the model's performance, after the training process had finished.

2.2.3. Training U-net

From the available CNNs, we chose the U-net architecture. This network is able to recognize patterns at multiple spatial scales, making it a suitable network for vegetation and habitat type mapping (Cheng et al., 2024; Kattenborn et al., 2019). Moreover, U-net can work well with relatively small training data sets (Gonzalez-Perez et al., 2022). We implemented U-net using the PyTorch machine learning framework version 1.9 (Paszke et al., 2019). Details about the implemented architecture can be found in Table S4. Next, we trained the network on a high-performance computing resource (GPU Tesla V100 with 32 GB memory) at the Royal Netherlands Institute for Sea Research. When loading the training data, we applied data augmentation techniques to artificially enlarge the training set. Each input image was randomly flipped horizontally or vertically (with a probability of 0.5 each) and rotated up to 180°. Moreover, because the classes were not equally balanced in the training set, we added weights to the classes (Table S5). These weight values were inversely proportional to the relative occurrence of the classes in the training set, awarding the network more for correctly predicting underrepresented classes (e.g. fresh water) than for overrepresented classes (e.g. grass). During the training in each *epoch* (i.e. training set iteration), the network processed the full set of training images in *batches* (i.e. samples) (Kattenborn et al., 2021). Due to memory limitations and our relatively large image size, we set the batch size to one. The network thus predicted one image at a time, compared the prediction to the expected outcome, calculated the training loss and updated its internal model parameters. To compute the training loss and the validation loss, we used the function *weighted cross-entropy* and minimized it via *stochastic gradient descent* optimization (Aurelio et al., 2019). To guide the learning process, we adjusted the learning rate over time (Yedida and Saha, 2019). It was initially set at 0.01 and reduced by a factor 10 each time the validation loss did not improve for 100 epochs. This strategy ensured larger parameter updates in the early stages and more refined adjustments as training progressed. When the validation loss showed no improvement for 150 consecutive epochs, indicating stabilization of validation loss (Fig. S2), the training process stopped. To test the usefulness of our input data layers, we repeatedly trained the network using multiple combinations of layers. We started with RGB imagery only (Model 5) and then added step by step the following bands: near-infrared (Model 4), distance to sea (Model 3), digital surface model (Model 2), and canopy height (Model 1). This resulted in five trained networks. Finally, we evaluated the performance of each trained network on the annotated images of the test set (Fig. S3 and S4).

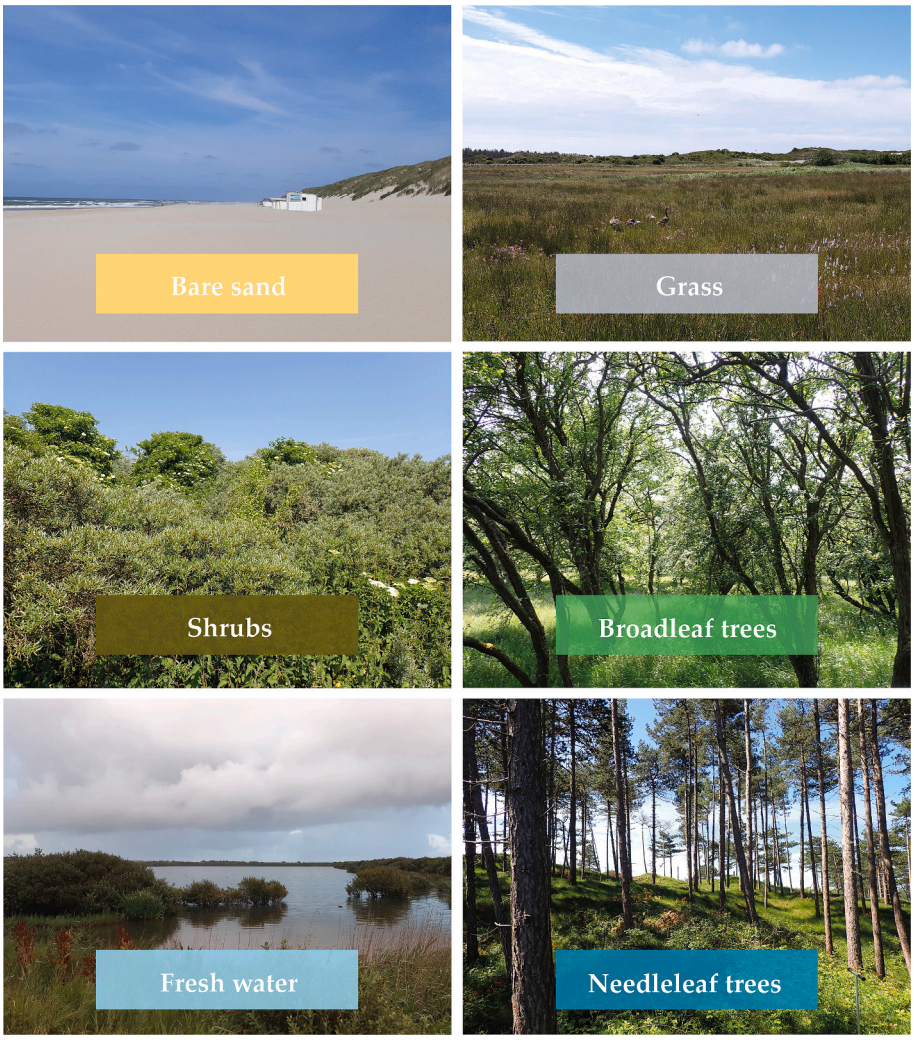

Fig. 2. The six coastal dune habitat classes in the Netherlands seen from the ground.

2.3. Evaluation metrics

The performance of the models was compared using five commonly used metrics to evaluate semantic segmentation (Cheng et al., 2024; Ribeiro et al., 2023; Yu et al., 2018): accuracy, recall, precision, F1-score and Intersection over Union (Table 1). These metrics range between 0 and 100, with a higher value indicating better performance. Specifically, they are defined as: *accuracy* reflects the overall correctness of the model's predictions, *recall* indicates how often the true class (i.e. like the class is segmented in the test set) matches the predicted class, *precision* shows how often the predicted class matches the true class, *F1-score* is the harmonic mean of recall and precision (Foody, 2023), and the *Intersection over Union* quantifies the percentage of overlap between the true and predicted mask (van Beers et al., 2019).

2.4. Ground truthing

In addition, we examined how well our predictions matched in-field observations. For this purpose, we used our ground truthing dataset. In the summer of 2021, we had collected 499 habitat type observations (bare sand, grass, shrubs, broadleaf trees, needleleaf trees) and GPS points (Garmin GPSMAP 65 s; 1.8 m minimal accuracy) in the dunes across the Netherlands (Lansu et al., 2025). We chose 35 locations across the country with a balanced spatial distribution over the study area (Fig. S7). At each location, we walked cross-shore transects and observed the habitat type every 100 m. To compare these in-field observations with our U-net predictions, we predicted the habitat type around the GPS points in a 10*10 m area. From this area, we computed the modus (i.e. the most occurring class). To quantify the effect of difference in perspective - aerial versus ground-level view - we also visually classified the ground truthing points on the aerial imagery. This enabled us to compare three different classification methods: model prediction, visual interpretation of the aerial imagery, and ground observation.

2.5. Mapping

We used the best-performing model to classify the entire coastal dune landscape of the Netherlands. We georeferenced the resulting predictions using MATLAB's Mapping Toolbox version 24.2 (The MathWorks Inc., 2024a). Finally, we uploaded the georeferenced predictions in the Earth Engine app, using Earth Engine code editor (Gorelick et al., 2017).

3. Results

To compare the trained models, and thereby the added value of each data layer, we computed evaluation metrics based on the test set. In this section, we present these metrics per model (Table 2) as an overall indication of model performance. Comparing these metrics among models gives an indication of the overall added value of each data layer. Next, we present these metrics per model per class, showing to what extend each class benefited from the addition of input data layers.

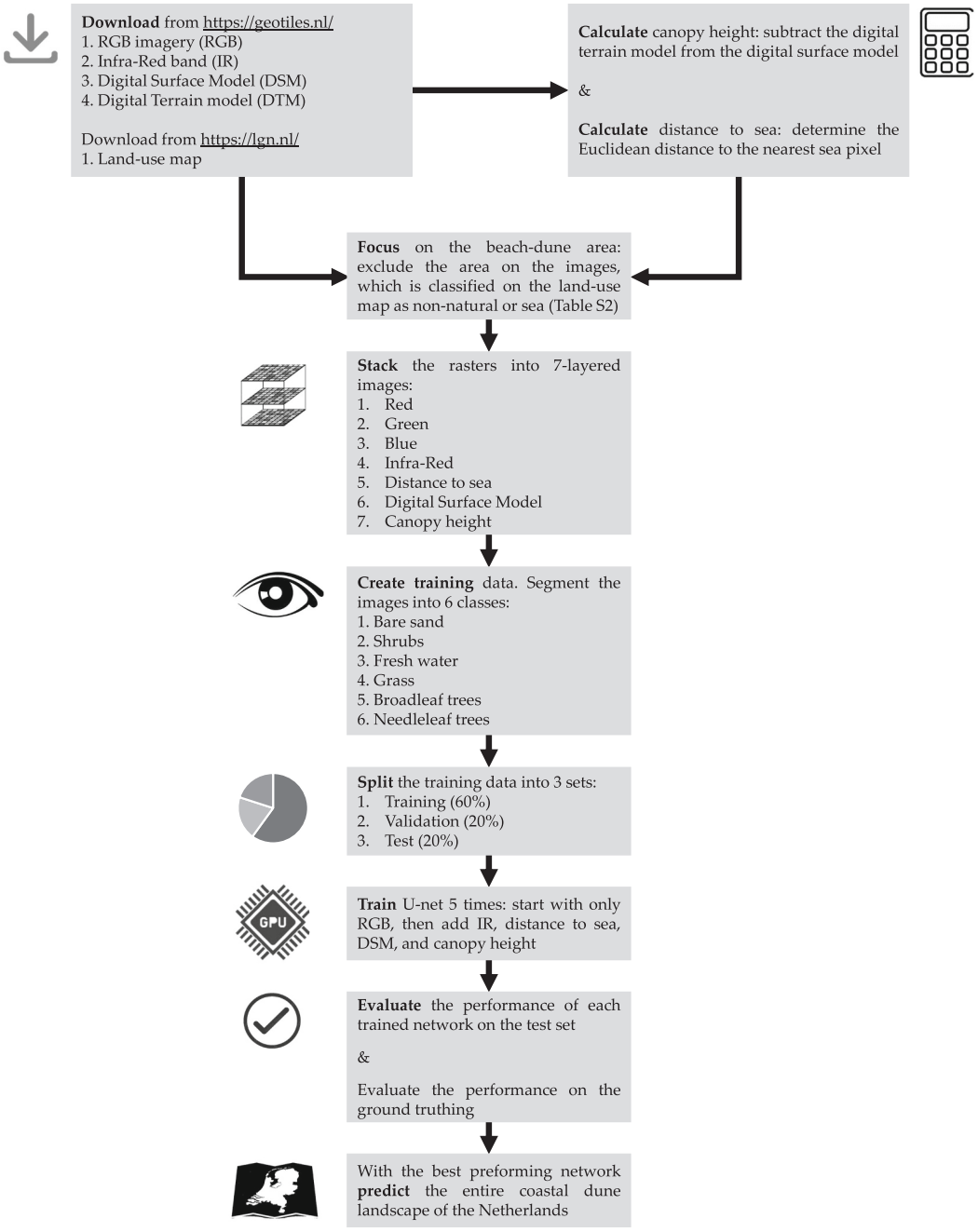

Fig. 3. The steps of our applied methodology.

Finally, we present the in-field accuracy of our best-performing model based on 499 in-field observations.

3.1. Overall model performance

Model 5, trained solely on RGB data, achieved an average recall of 79.5 % and a precision of 70.4 % (Table 2). Adding near-infrared in model 4 slightly improved performance, with an average recall of 81.6 % and precision of 72.8 %. In contrast, incorporating distance to sea in model 3 gave a more ambiguous result: recall improved slightly to 82.1 %, but precision decreased to 71.3 %. Including the digital surface model in model 2 improved performance again, increasing recall to 86.4 % and precision to 78.2 %. Finally, including also canopy height in model 1 yielded the best performance with an average recall of 87.7 % and precision of 80.1 %. Apart from scoring the highest overall metrics, model 1 also learned the 'fastest', as it required the fewest training epochs to saturate validation loss (Fig. S2).

3.2. Model performance per class

The model performance was further compared using the recall values per class (Fig. 4, S3, S4). Model 1 (all layers included) consistently performed best across all classes, with the highest recall for bare sand (97.0 %), followed by fresh water (94.0 %), broadleaf trees (88.9 %), needleleaf trees (84.7 %), grass (81.4 %), and shrubs (80.3 %). Although model 1 predicted each class better than the other models, the magnitude of improvement was variable, when comparing model 1 and 5. For four classes – bare sand, grass, broadleaf, and needleleaf trees – the recall difference between model 1 and model 5 was relatively small (2.5 to 7.6 percentage points). Hence, often similar predictions were

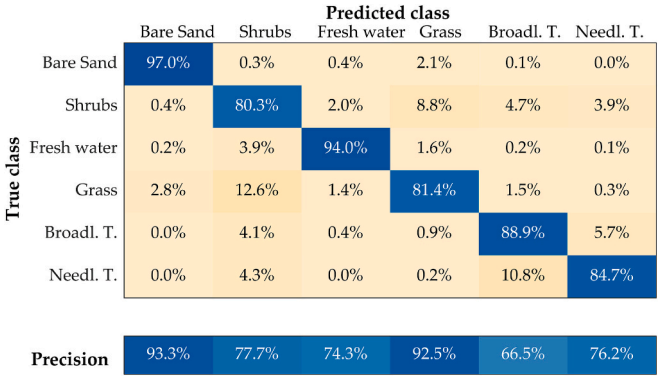

Fig. 4. The normalized confusion matrix of model 1, trained on all input data (Table 2), based on the predictions of the test set. The recall is presented in the diagonal of the matrix, the precision in the table below.

generated by all models, when the image predominantly consisted of these four habitat classes (example: Fig. S5). In contrast, the recall of the other two classes – fresh water and shrubs (15.1 and 15.7 percentage points difference between model 1 and 5, respectively) – differed substantially. Near-infrared mainly contributed to the improvement of fresh water classification (example: Fig. 5), while mostly elevation data (digital surface model and canopy height) contributed to the improvement of shrubs classification by reducing the confusion between shrubs and broadleaf trees (example: Fig. S6).

3.3. Ground truthing

Apart from testing the model performance on annotated imagery, we also compared predictions of our best-performing model with 499 in-field observations (Fig. S7 and S8). On the country-scale (432 km of coastline (Brand et al., 2022)), we found no spatial pattern in model performance (Fig. S7). The accuracy of the ground truthing predictions was 87.5 %, the average recall 73.7 %, and the average precision 61.7 % (Fig. S8). The class needleleaf trees had the highest recall (88.2 %), followed by bare sand (80.0 %), shrubs (71.4 %), grass (64.6 %), and broadleaf trees (64.2 %). It should be noted that the classes were not equally balanced: while no ground truthing points were taken in fresh water, most points were taken in grassland (288 from 499 observations). This class thus largely determined the overall accuracy and overall recall.

3.4. Aerial versus ground-level view

We compared three methods of classification: the model prediction (model 1), the visual interpretation of the aerial imagery, and the ground observation (Fig. S9). At the locations of the ground truthing points, the model predictions were more in agreement with the visual assessment (86.6 % overall recall) than with the ground observations (68.7 % overall recall). Lastly, when comparing the differing perspectives directly, we find a moderate agreement (73.7 % overall recall) between the ground truthing and the visual assessment.

3.5. Mapping

Using model 1 (all data layers included), we classified the entire Dutch coastal dune system at 25 cm resolution. From the total beach-dune area (562 km^2), we found that bare sand covered 20 %, shrubs 21 %, fresh water 12 %, grass 30 %, broadleaf trees 11 %, and needleleaf trees 5 %. Scan the QR-code in Fig. 6 to view the map in the Earth Engine app.

4. Discussion

Here, we investigated how accurately a CNN can map coastal dune habitats on high-resolution imagery at a national scale (>500 km^2). With our method we find that training the network using RGB data alone already provides a level of accuracy (92.4 %) suitable to make a first estimate of habitat diversity. Hence, using RGB data could be satisfactory in areas where only aerial footage is available. Nevertheless, our work also highlights that the addition of more data layers – in particular

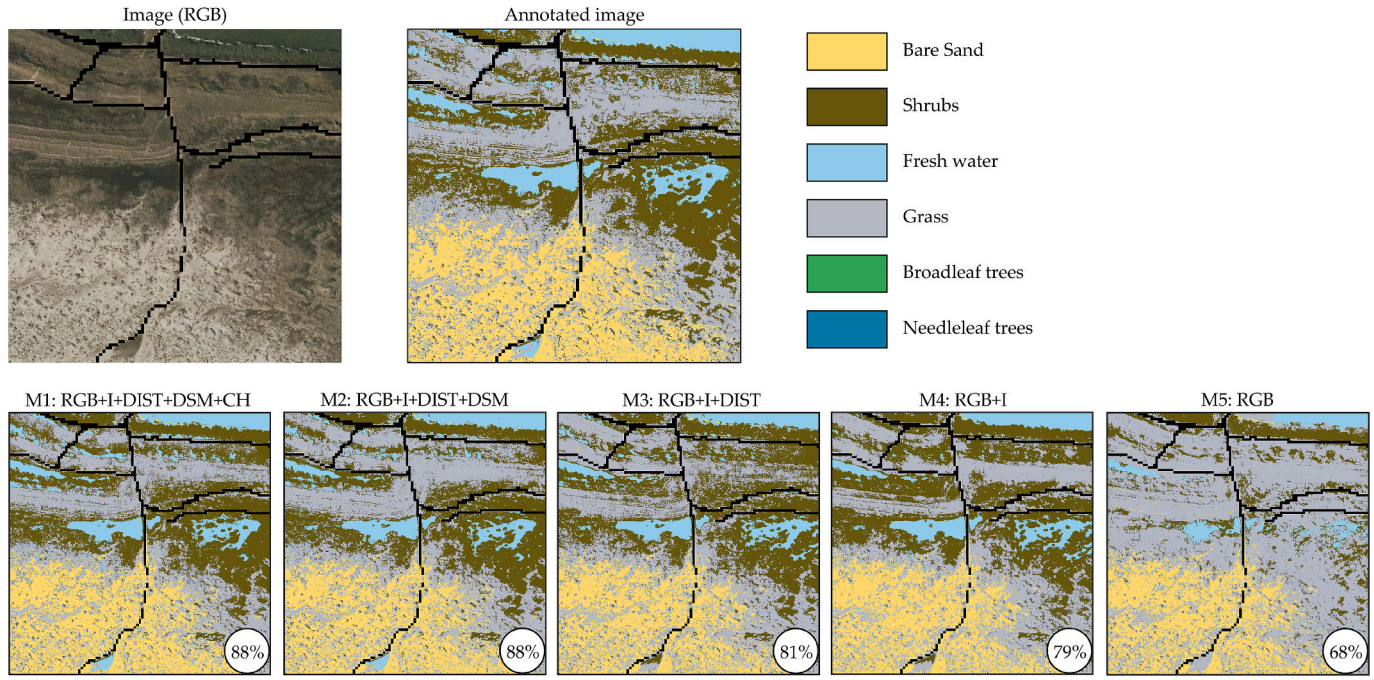

Fig. 5. An example of an image from the test set, the annotated image, and the corresponding model predictions. The black pixels indicate other land-use (filtered out in advance) and the percentages indicate overall recall of the model predictions. The example illustrates that including near-infrared improves the fresh water classification.

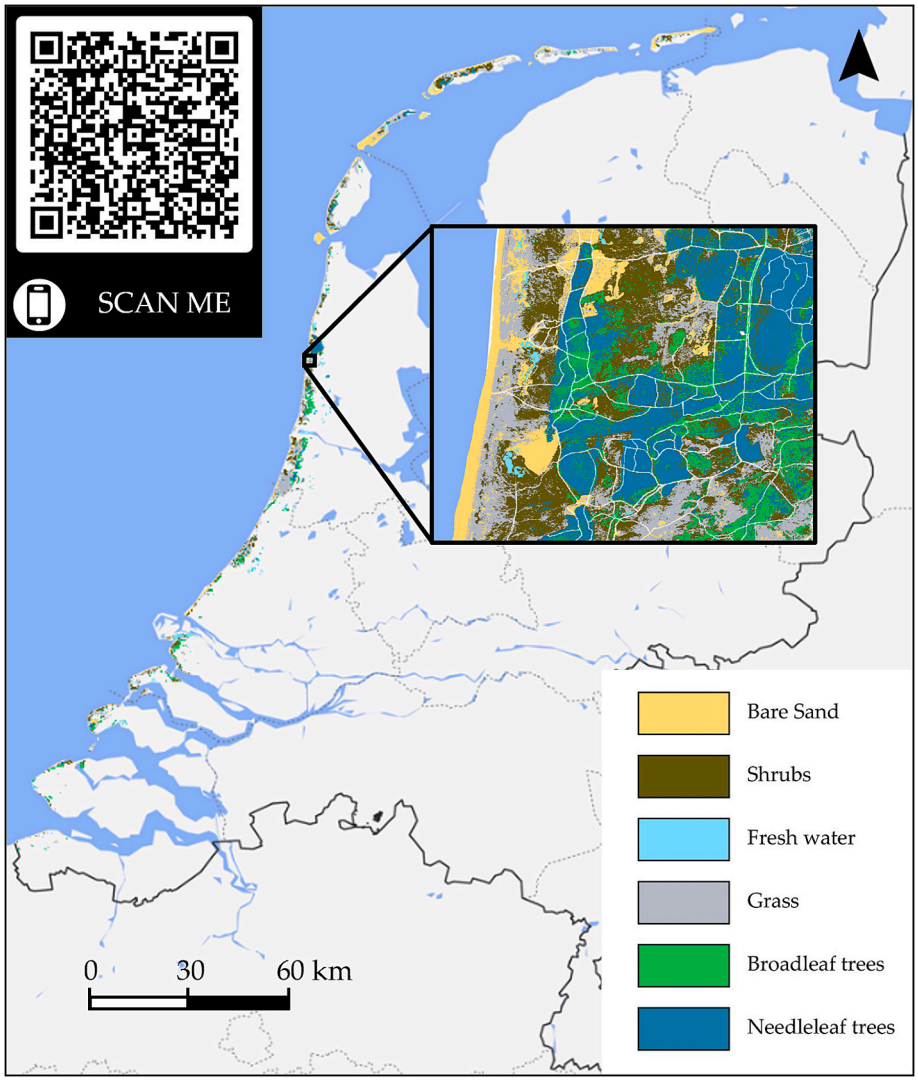

Fig. 6. The predicted habitat classes in the Dutch coastal dunes for the year 2020. Use the QR-code or this link https://liquid-optics-366616.projects.earthengine.app/view/coastal-habitats to visit the Earth Engine app, where you can zoom in on the map.

Table 1
The calculation of the evaluation metrics used in this study, where TP is true positives, TN true negatives, FP false positives, and FN false negatives.

Accuracy	(TP + TN) / (TP + TN + FP + FN)
Recall	TP / (TP + FN)
Precision	TP / (TP + FP)
F1 score	2 * precision * recall / (precision + recall)
Intersection over Union	TP / (TP + FP + FN)

near-infrared data, a digital surface model and a canopy height map - further improves the prediction accuracy. When the network is trained on all data layers, a high level of accuracy can be obtained (95.0 %), which enables precise assessments of habitat diversity and spatial organization (James et al., 2024), crucial for better understanding ecological status, functioning and resilience of coastal dunes (Acosta et al., 2009; Malavasi et al., 2018; Ryan et al., 2024; Sperandii et al., 2019).

Table 2
Evaluation metrics (%), based on how the models predicted the test set. The term *overall* implies that the metric is about the total amount of (in)correctly predicted pixels across all classes. Because false negatives and false positives balance out across all classes, overall recall is exactly equal to overall precision. We therefore only report overall recall. For the average and mean metrics, we computed the index per class and took the average of these values.

Model	Input data	Overall Accuracy	Overall Recall	Average Recall	Average Precision	F1-score	Mean IoU
1	RGB + I + Dist. to sea + DSM + Canopy height	95.0	85.0	87.7	80.1	83.7	71.9
2	RGB + I + Dist. to sea + DSM	94.7	84.0	86.4	78.2	82.1	69.7
3	RGB + I + Dist. to sea	93.1	79.3	82.1	71.3	76.3	61.6
4	RGB + I	92.9	78.7	81.6	72.8	77.0	62.7
5	RGB	92.4	77.3	79.5	70.4	74.6	59.8

4.1. The value of additional input data

In our analysis, we find that using RGB data alone already provides an acceptable level of accuracy, however, the addition of data layers further improves the prediction accuracy. This is in line with comparable studies, in which U-net was trained with high-resolution aerial imagery, but with a simpler aim: the segmentation of water bodies on aerial imagery in wetlands (Hu et al., 2021) and in diverse environments (Wieland et al., 2023). These studies also found that the model performed well when solely trained on RGB, but the accuracy increased when near-infrared and elevation data were added (Hu et al., 2021; Wieland et al., 2023). Specifically, we find that the addition of near-infrared data largely improves the recognition of freshwater, while the addition of the elevation data (digital surface model and canopy height) strongly improves the network's ability to differentiate between shrubs and trees. The latter is in line with a case study in the Belgian coastal dunes (Kempeneers et al., 2009). In contrast to the other data layers, distance to sea did not have a clear added value, as it did not improve all evaluation metrics (Table 1). Hence, we conclude that the use of multispectral images can strongly enhance predictions in ecosystems that include freshwater bodies, while the addition of elevation data can greatly improve predictions in ecosystems containing both shrubs and trees.

4.2. Ground-level accuracy

To obtain an estimate for ground-level accuracy, we used our ground truthing set of 499 in-field observations. In addition, we visually assessed the ground truthing points on the aerial imagery to compare the ground perspective with the aerial perspective. We then found that the model predictions were more in agreement with the visual assessment (86.6 % overall recall) than with the ground truthing (68.7 % overall recall). This discrepancy can firstly be related to the fact that the annotated imagery, on which the model was trained, was also visually assessed. It can therefore be expected that model predictions match better the visual assessment than the ground observations. Secondly, this discrepancy can be related to the perspective, as we found that in 26 % of the cases, the ground observation differed from our visual assessment. Thirdly, the moment of observation differed: the ground truthing (2021) was collected a year after the aerial imagery and the elevation data (2020) were collected. Lastly, we took a point observation with a GPS in the field, which had a precision of 1.8 m. This type of field data does not allow for a spatial explicit link with the remote sensing data, which is a common problem with in-situ observations (Anderson, 2018; Kattenborn and Schmidtlein, 2019; Leitão et al., 2018). In particular in the heterogeneous coastal dunes, it may lead to spatial mismatches. Despite these methodological differences in perspective (aerial versus ground based), time (2020 versus 2021), and sampling method (slightly deviating sampling location), our model predictions still largely align with the ground observations.

4.3. A labour-efficient way of mapping

Besides yielding accurate predictions, our method of automated image analysis is also a labour-efficient way to map dune habitats. Since the input data was freely available, the most tedious step was the creation of training data. This step took one person approximately seven working days. Moreover, this effort does not have to be repeated to classify imagery of another year. Instead, the trained network can then be used as a starting point and only a new test set (88 annotated images of 512 × 512 m) is required to compute how well the model performs when classifying the new imagery. In case the model performance does not meet prior set criteria, extra training data can be generated to further train the model. As such, the required additional labour remains within the timespan of a few working days. In contrast, with a field-based approach, examining the complete study area would take over a year, and revisiting the area in another year would take equally long. Nevertheless, our rapid remote sensing-based approach is not able to identify habitat classes at the same level of detail as a field-based study would. Hence, we argue that our novel approach can complement – but not replace – in-field observations by providing a full-coverage picture within a short amount of time and at relatively low costs. Moreover, with the generated map, more informed decisions could be taken on where a field visit is most effective.

5. Conclusions

While vegetation classification with CNN is widely used in forestry and agriculture, its applications in coastal systems and conservation monitoring remained scarce and limited to small-scale studies (Attri et al., 2023; Kattenborn et al., 2021). This underutilization is surprising given the dynamic nature of coastal areas, which could greatly benefit from improved monitoring techniques. In this study, we showcase how automated analysis - using multispectral imagery, distance to sea, digital surface model, and canopy height model - can be applied to accurately map habitats in the coastal dunes on a national scale. Moreover, as habitat and species diversity are intrinsically linked (Lansu et al., 2025), our results demonstrate how automated image analysis can enable large-scale monitoring of biodiversity. Similar upscaling approaches could revolutionize the monitoring of other coastal ecosystems, such as shellfish reefs (Ridge et al., 2020), wetlands (DeLancey et al., 2020) and seagrass meadows (James et al., 2024; Langlois et al., 2023). Given the vital ecosystem services that coastal systems provide, their preservation is paramount. Habitat monitoring across space and time can play an essential role in the development of strategic management to ensure their long-term preservation.

Funding

EL was funded by NWO-LLDD grant 17595; VR was funded by NWO-Veni grant VI.Veni.212.059; TH was supported by NWO/TTW-Vidi grant 16588; RKJ was supported by a MSCA European Postdoctoral Fellowship (Project 101060342 – SCaLED); and MJAC by NWO-WOTRO 481.20.04.

CRediT authorship contribution statement

Eva M. Lansu: Writing – review & editing, Writing – original draft, Visualization, Methodology, Investigation, Formal analysis, Conceptualization. **Valérie C. Reijers:** Writing – review & editing, Supervision, Funding acquisition, Conceptualization. **Freek Daniëls:** Writing – review & editing, Software, Methodology. **Rebecca James:** Writing – review & editing, Methodology. **Marjolijn J.A. Christianen:** Writing – review & editing, Methodology. **Tjisse van der Heide:** Writing – review & editing, Supervision, Funding acquisition, Conceptualization.

Declaration of competing interest

The authors declare that they have no known competing financial interests or personal relationships that could have appeared to influence the work reported in this paper.

Acknowledgments

We would like to thank Hans Malschaert for his help with the use of the high-performance computing cluster at NIOZ.

Appendix A. Supplementary data

Supplementary data to this article can be found online at https://doi.org/10.1016/j.ecoinf.2025.103444.

Data availability

Data and script analyses presented in this study are deposited in Zenodo (https://doi.org/10.5281/zenodo.14197160).

References

Acosta, A., Carranza, M.L., Izzi, C.F., 2009. Are there habitats that contribute best to plant species diversity in coastal dunes? Biodivers. Conserv. 18 (4), 1087–1098. https://doi.org/10.1007/s10531-008-9454-9.

Alberdi, I., Nunes, L., Kovac, M., Bonheme, I., Cañellas, I., Rego, F.C., Dias, S., Duarte, I., Notarangelo, M., Rizzo, M., Gasparini, P., 2019. The conservation status assessment of natura 2000 forest habitats in Europe: capabilities, potentials and challenges of national forest inventories data. Ann. For. Sci. 76 (2). https://doi.org/10.1007/s13595-019-0820-4.

Anderson, C.B., 2018. Biodiversity monitoring, earth observations and the ecology of scale. Ecol. Lett. 21 (10), 1572–1585. https://doi.org/10.1111/ele.13106.

Arens, S.M., de Vries, S., Geelen, L.H., Ruessink, G., van der Hagen, H.G., Groenendijk, D., 2020. Comment on 'is "re-mobilisation" nature restoration or nature destruction? A commentary' by I. Delgado-Fernandez, R.G.D. Davidson-Arnott & P.A. Hesp. J. Coast. Conserv. 24 (2), 17–20. https://doi.org/10.1007/s11852-020-00731-1.

Attri, I., Awasthi, L.K., Sharma, T.P., Rathee, P., 2023. A review of deep learning techniques used in agriculture. Eco. Inform. 77, 102217. https://doi.org/10.1016/j.ecoinf.2023.102217.

Aurelio, Y.S., de Almeida, G.M., de Castro, C.L., Braga, A.P., 2019. Learning from imbalanced data sets with weighted cross-entropy function. Neural. Process. Lett. 50 (2), 1937–1949. https://doi.org/10.1007/s11063-018-09977-1.

Azarafza, M., Azarafza, M., Akgün, H., Atkinson, P.M., Derakhshani, R., 2021. Deep learning-based landslide susceptibility mapping. Sci. Rep. 11 (1), 1–16. https://doi.org/10.1038/s41598-021-03585-1.

Barbier, E.B., Hacker, S.D., Kennedy, C., Koch, E.W., Stier, A.C., Silliman, B.R., 2011. The value of estuarine and coastal ecosystem services. Ecol. Monogr. 81 (2), 169–193.

van Beers, F., Lindström, A., Okafor, E., Wiering, M.A., 2019. Deep neural networks with intersection over union loss for binary image segmentation. Intern. Confer. Pattern Recogn. Appl. Method. 1, 438–445. https://doi.org/10.5220/0007347504380445.

BIJ12, 2021. Werkwijze Monitoring en Beoordeling Natuurnetwerk en Natura 2000. https://www.bij12.nl/onderwerpen/natuur-en-landschap/monitoring-en-natuurinformatie/.

Bird, T.L.F., Dorman, M., Ramot, A., Bouskila, A., Bar Kutiel, P., Groner, E., 2017. Shrub encroachment effects on habitat heterogeneity and beetle diversity in a Mediterranean coastal dune system. Land Degrad. Dev. 28 (8), 2553–2562. https://doi.org/10.1002/ldr.2807.

Brand, E., Ramaekers, G., Lodder, Q., 2022. Dutch experience with sand nourishments for dynamic coastline conservation – An operational overview. Ocean Coast. Manag. 217, 106008. https://doi.org/10.1016/j.ocecoaman.2021.106008.

Chapin, F.S., Sala, O.E., Burke, I.C., Phillip Grime, J., Hooper, D.U., Lauenroth, W.K., Lombard, A., Mooney, H.A., Mosier, A.R., Naeem, S., Pacala, S.W., Roy, J., Steffen, W.L., Tilman, D., 1998. Ecosystem consequences of changing biodiversity. BioScience 48 (1), 45–52. https://doi.org/10.2307/1313227.

Cheng, J., Deng, C., Su, Y., An, Z., Wang, Q., 2024. Methods and datasets on semantic segmentation for unmanned aerial vehicle remote sensing images: a review. ISPRS J. Photogramm. Remote Sens. 211, 1–34. https://doi.org/10.1016/j.isprsjprs.2024.03.012.

Choudhary, K., DeCost, B., Chen, C., Jain, A., Tavazza, F., Cohn, R., Park, C.W., Choudhary, A., Agrawal, A., Billinge, S.J.L., Holm, E., Ong, S.P., Wolverton, C., 2022. Recent advances and applications of deep learning methods in materials science. npj Comput. Mater. 8 (1), 59. https://doi.org/10.1038/s41524-022-00734-6.

DeLancey, E.R., Simms, J.F., Mahdianpari, M., Brisco, B., Mahoney, C., Kariyeva, J., 2020. Comparing deep learning and shallow learning for large-scale wetland classification in Alberta, Canada. Remote Sens 12 (1). https://doi.org/10.3390/RS12010002.

Delbosc, P., Lagrange, I., Rozo, C., Bensettiti, F., Bouzillé, J.B., Evans, D., Lalanne, A., Rapinel, S., Bioret, F., 2021. Assessing the conservation status of coastal habitats under article 17 of the EU habitats directive. Biol. Conserv. 254, 108935. https://doi.org/10.1016/j.biocon.2020.108935.

Delgado-Fernandez, I., O'Keeffe, N., Davidson-Arnott, R.G.D., 2019. Natural and human controls on dune vegetation cover and disturbance. Sci. Total Environ. 672, 643–656. https://doi.org/10.1016/j.scitotenv.2019.03.494.

Drius, M., Jones, L., Marzialetti, F., de Francesco, M.C., Stanisci, A., Carranza, M.L., 2019. Not just a sandy beach. The multi-service value of Mediterranean coastal dunes. Sci. Total Environ. 668, 1139–1155. https://doi.org/10.1016/j.scitotenv.2019.02.364.

Eelbode, T., Sinonquel, P., Maes, F., Bisschops, R., 2021. Pitfalls in training and validation of deep learning systems. Best Pract. Res. Clin. Gastroenterol. 52–53, 101712. https://doi.org/10.1016/j.bpg.2020.101712.

Foody, G.M., 2023. Challenges in the real world use of classification accuracy metrics: from recall and precision to the Matthews correlation coefficient. PLoS One 18 (10), 1–27. https://doi.org/10.1371/journal.pone.0291908.

Gao, J., Kennedy, D.M., Konlechner, T.M., 2020. Coastal dune mobility over the past century: A global review. Prog. Phys. Geogr. 44 (6), 814–836. https://doi.org/10.1177/0309133320919612.

Garcia-Garcia, A., Orts-Escolano, S., Oprea, S., Villena-Martinez, V., Garcia-Rodriguez, J., 2017. A review on deep learning techniques applied to semantic segmentation. ArXiv (Preprint) 1–23. http://arxiv.org/abs/1704.06857.

Gonzalez-Perez, A., Abd-Elrahman, A., Wilkinson, B., Johnson, D.J., Carthy, R.R., 2022. Deep and machine learning image classification of coastal wetlands using unpiloted aircraft system multispectral images and lidar datasets. Remote Sens 14 (16), 3937. https://doi.org/10.3390/rs14163937.

Gorelick, N., Hancher, M., Dixon, M., Ilyushchenko, S., Thau, D., Moore, R., 2017. Google earth engine: planetary-scale geospatial analysis for everyone. Remote Sens. Environ. 202, 18–27. https://doi.org/10.1016/j.rse.2017.06.031.

Hesp, P., 2002. Foredunes and blowouts: initiation, geomorphology and dynamics. Geomorphology 48, 245–268.

Hilton, M.J., 2006. The loss of New Zealand's active dunes and the spread of marram grass (Ammophila arenaria). N. Z. Geogr. 62 (2), 105–120. https://doi.org/10.1111/j.1745-7939.2006.00054.x.

Hu, Q., Woldt, W., Neale, C., Zhou, Y., Drahota, J., Varner, D., Bishop, A., LaGrange, T., Zhang, L., Tang, Z., 2021. Utilizing unsupervised learning, multi-view imaging, and CNN-based attention facilitates cost-effective wetland mapping. Remote Sens. Environ. 267, 112757. https://doi.org/10.1016/j.rse.2021.112757.

Jackson, D., Cooper, J.A.G., 2011. Coastal dune fields in Ireland: rapid regional response to climatic change. J. Coast. Res. 64, 293–297.

Jackson, D., Costas, S., González-Villanueva, R., Cooper, A., 2019. A global 'greening' of coastal dunes: An integrated consequence of climate change? Glob. Planet. Chang. 182, 103026. https://doi.org/10.1016/j.gloplacha.2019.103026.

James, R.K., Daniels, F., Chauhan, A., Wicaksono, P., Hafizt, M., Harahap, S.D., Christianen, M.J.A., 2024. Monitoring vegetation patterns and their drivers to infer resilience: automated detection of vegetation and megaherbivores from drone imagery using deep learning. Eco. Inform. 81, 102580. https://doi.org/10.1016/j.ecoinf.2024.102580.

Kattenborn, T., Schmidtlein, S., 2019. Radiative transfer modelling reveals why canopy reflectance follows function. Sci. Rep. 9 (1), 1–10. https://doi.org/10.1038/s41598-019-43011-1.

Kattenborn, T., Eichel, J., Fassnacht, F.E., 2019. Convolutional neural networks enable efficient, accurate and fine-grained segmentation of plant species and communities from high-resolution UAV imagery. Sci. Rep. 9 (1), 1–9. https://doi.org/10.1038/s41598-019-53797-9.

Kattenborn, T., Leitloff, J., Schiefer, F., Hinz, S., 2021. Review on convolutional neural networks (CNN) in vegetation remote sensing. ISPRS J. Photogramm. Remote Sens. 173, 24–49. https://doi.org/10.1016/j.isprsjprs.2020.12.010.

Kempeneers, P., Deronde, B., Provoost, S., Houthuys, R., 2009. Synergy of airborne digital camera and lidar data to map coastal dune vegetation. J. Coast. Res. 53, 73–82. https://doi.org/10.2112/SI53-009.1.

Laignel, B., Vignudelli, S., Almar, R., Becker, M., Bentamy, A., Benveniste, J., Birol, F., Frappart, F., Idier, D., Salameh, E., Passaro, M., Menende, M., Simard, M., Turki, E.I., Verpoorter, C., 2023. Observation of the coastal areas, estuaries and deltas from space. Surv. Geophys. 44 (5), 1309–1356. https://doi.org/10.1007/s10712-022-09757-6.

Lane, C., Wright, S.J., Roncal, J., Maschinski, J., 2008. Characterizing environmental gradients and their influence on vegetation zonation in a subtropical coastal sand dune system. J. Coast. Res. 24 (4), 213–224. https://doi.org/10.2112/07-0853.1.

Langlois, L.A., Collier, C.J., McKenzie, L.J., 2023. Subtidal seagrass detector: development of a deep learning seagrass detection and classification model for seagrass presence and density in diverse habitats from underwater photoquadrats. Front. Mar. Sci. 10, 1–13. https://doi.org/10.3389/fmars.2023.1197695.

Lansu, E.M., Reijers, V., Höfer, S., Luijendijk, A., Rietkerk, M., Wassen, M., Lammerts, E. J., van der Heide, T., 2024. A global analysis of how human infrastructure squeezes sandy coasts. Nat. Commun. 15 (1), 432. https://doi.org/10.1038/s41467-023-44659-0.

Lansu, E.M., Fischman, H., Angelini, C., Hijner, N., Geelen, L., Groenendijk, D., Höfer, S., Kooijman, A., Rietkerk, M., Tonkens, S., de Vries, S., Wassen, M., van Weerlee, E., Wille, D., Reijers, V., van der Heide, T., 2025. How human infrastructure threatens biodiversity by squeezing sandy coasts. Curr. Biol. https://doi.org/10.1016/j.cub.2025.09.027.

Lecun, Y., Bengio, Y., Hinton, G., 2015. Deep learning. Nature 29 (7553), 1–73. https://doi.org/10.1038/nature14539.

Leitão, P.J., Schwieder, M., Pötzschner, F., Pinto, J.R.R., Teixeira, A.M.C., Pedroni, F., Sanchez, M., Rogass, C., van der Linden, S., Bustamante, M.M.C., Hostert, P., 2018. From sample to pixel: multi-scale remote sensing data for upscaling aboveground carbon data in heterogeneous landscapes. Ecosphere 9 (8), e02298. https://doi.org/10.1002/ecs2.2298.

Lu, Y., Yuan, J., Lu, X., Su, C., Zhang, Y., Wang, C., Cao, X., Li, Q., Su, J., Ittekkot, V., Garbutt, R.A., Bush, S., Fletcher, S., Wagey, T., Kachur, A., Sweijd, N., 2018. Major threats of pollution and climate change to global coastal ecosystems and enhanced management for sustainability. Environ. Pollut. 239, 670–680. https://doi.org/10.1016/j.envpol.2018.04.016.

Luijendijk, A., Hagenaars, G., Ranasinghe, R., Baart, F., Donchyts, G., Aarninkhof, S., 2018. The state of the world's beaches. Sci. Rep. 8 (1), 1–11. https://doi.org/10.1038/s41598-018-24630-6.

Maccherini, S., Bacaro, G., Tordoni, E., Bertacchi, A., Castagnini, P., Foggi, B., Gennai, M., Mugnai, M., Sarmati, S., Angiolini, C., 2020. Enough is enough? Searching for the optimal sample size to monitor European habitats: a case study from coastal sand dunes. Diversity 12 (4), 138. https://doi.org/10.3390/D12040138.

Malavasi, M., Bartak, V., Carranza, M.L., Simova, P., Acosta, A., 2018. Landscape pattern and plant biodiversity in Mediterranean coastal dune ecosystems: do habitat loss and

fragmentation really matter? J. Biogeogr. 45 (6), 1367–1377. https://doi.org/10.1111/jbi.13215.
Martínez, M.L., Psuty, N.P., Lubke, R.A., 2004. A perspective on coastal dunes. Ecol. Stud. 171, 3–10. https://doi.org/10.1007/978-3-540-74002-5_1.
McLachlan, A., 1991. Ecology of coastal dune fauna. J. Arid Environ. 21 (2), 229–243. https://doi.org/10.1016/s0140-1963(18)30684-0.
Melet, A., Teatini, P., Le Cozannet, G., Jamet, C., Conversi, A., Benveniste, J., Almar, R., 2020. Earth observations for monitoring marine coastal hazards and their drivers. Surv. Geophys. 41 (6), 1489–1534. https://doi.org/10.1007/s10712-020-09594-5.
Naumann, S., Noebel, R., Gaudillat, Z., Stein, U., Röschel, L., Ittner, S., McKenna, D., Staneva, A., Rutherford, C., Romão, C., 2020. State of nature in the EU: Results from reporting under the nature directives 2013-2018. In: EEA Report. EEA report. http://bookshop.europa.eu/ro/state-of-nature-in-the-eu-pbTHAK15002/?CatalogCategoryID=iEKep2Ix3hEAAAEud3kBgSLq.
Paszke, A., Gross, S., Massa, F., Lerer, A., Bradbury Google, J., Chanan, G., Killeen, T., Lin, Z., Gimelshein, N., Antiga, L., Desmaison, A., Xamla, A.K., Yang, E., Devito, Z., Raison Nabla, M., Tejani, A., Chilamkurthy, S., Ai, Q., Steiner, B., Chintala, S., 2019. PyTorch: An imperative style, high-performance deep learning library. Adv. Neural Inf. Proces. Syst. 32. In: https://proceedings.neurips.cc/paper_files/paper/2019/file/bdbca288fee7f92f2bfa9f7012727740-Paper.pdf.
Pérez-Carabaza, S., Boydell, O., O'Connell, J., 2021. Habitat classification using convolutional neural networks and multitemporal multispectral aerial imagery. J. Appl. Remote. Sens. 15 (04), 1–12. https://doi.org/10.1117/1.jrs.15.042406.
Petrova, P.G., de Jong, S.M., Ruessink, G., 2023. A global remote-sensing assessment of the Intersite variability in the greening of coastal dunes. Remote Sens 15 (6). https://doi.org/10.3390/rs15061491.
Pye, K., Blott, S.J., 2017. Evolution of a sediment-starved, over-stabilised dunefield: Kenfig burrows, South Wales, UK. J. Coast. Conserv. 21 (5), 685–717. https://doi.org/10.1007/s11852-017-0506-8.
Pye, K., Blott, S.J., Howe, M.A., 2014. Coastal dune stabilization in Wales and requirements for rejuvenation. J. Coast. Conserv. 18 (1), 27–54. https://doi.org/10.1007/s11852-013-0294-8.
Ribeiro, T.F.R., Silva, F., Moreira, J., Costa, R.L. de C., 2023. Burned area semantic segmentation: a novel dataset and evaluation using convolutional networks. ISPRS J. Photogramm. Remote Sens. 202, 565–580. https://doi.org/10.1016/j.isprsjprs.2023.07.002.
Ridge, J.T., Gray, P.C., Windle, A.E., Johnston, D.W., 2020. Deep learning for coastal resource conservation: automating detection of shellfish reefs. Remote Sens. Ecol. Conserv. 6 (4), 431–440. https://doi.org/10.1002/rse2.134.
van Rooijen, N.M., de Keersmaecker, W., Ozinga, W.A., Coppin, P., Hennekens, S.M., Schaminée, J.H.J., Somers, B., Honnay, O., 2015. Plant species diversity mediates ecosystem stability of natural dune grasslands in response to drought. Ecosystems 18 (8), 1383–1394. https://doi.org/10.1007/s10021-015-9905-6.
Röschel, L., Noebel, R., Stein, U., Naumann, S., Romão, C., Tryfon, E., Gaudillat, Z., Roscher, S., Moser, D., Ellmauer, T., Löhnertz, M., Halada, L., Staneva, A., Rutherford, C., 2020. State of Nature in the EU - Methodological Paper. http://bd.eionet.europa.eu.
Ruocco, M., Bertoni, D., Sarti, G., Ciccarelli, D., 2014. Mediterranean coastal dune systems: which abiotic factors have the most influence on plant communities? Estuar. Coast. Shelf Sci. 149, 213–222. https://doi.org/10.1016/j.ecss.2014.08.019.
Ryan, C., Buckley, H.L., Bishop, C.D., Hinchliffe, G., Case, B.C., 2024. Quantifying vegetation cover on coastal active dunes using nationwide aerial image analysis. Remote Sens. Ecol. Conserv. 11 (1), 40–57. https://doi.org/10.1002/rse2.410.
Sperandii, M.G., Bazzichetto, M., Acosta, A.T.R., Barták, V., Malavasi, M., 2019. Multiple drivers of plant diversity in coastal dunes: A Mediterranean experience. Sci. Total Environ. 652, 1435–1444. https://doi.org/10.1016/j.scitotenv.2018.10.299.
Sperandii, M.G., Barták, V., Carboni, M., Acosta, A.T.R., 2021. Getting the measure of the biodiversity crisis in Mediterranean coastal habitats. J. Ecol. 109 (3), 1224–1235. https://doi.org/10.1111/1365-2745.13547.
The MathWorks Inc, 2024a. Mapping Toolbox (24.2). https://nl.mathworks.com/help/releases/R2024b/map/.
The MathWorks Inc, 2024b. Statistics and Machine Learning Toolbox (24.2). https://www.mathworks.com.
Vitousek, S., Buscombe, D., Vos, K., Barnard, P.L., Ritchie, A.C., Warrick, J.A., 2023. The future of coastal monitoring through satellite remote sensing. Cambridge Prisms: Coast. Futur. 1 (e10), 1–18. https://doi.org/10.1017/cft.2022.4.
Wieland, M., Martinis, S., Kiefl, R., Gstaiger, V., 2023. Semantic segmentation of water bodies in very high-resolution satellite and aerial images. Remote Sens. Environ. 287, 113452. https://doi.org/10.1016/j.rse.2023.113452.
Yedida, R., Saha, S., 2019. A novel adaptive learning rate scheduler for deep neural networks. ArXiv 1–21, 1902.07399v2.
Yu, H., Yang, Z., Tan, L., Wang, Y., Sun, W., Sun, M., Tang, Y., 2018. Methods and datasets on semantic segmentation: a review. Neurocomputing 304, 82–103. https://doi.org/10.1016/j.neucom.2018.03.037.